Eighth Australasian Fluid Mechanics
Conference, University of Newcastle,
N.S.W., 28 November/2 December 1983.

FINITE ELEMENT STUDY OF SOME FLOW PROBLEMS WITH THERMALLY INDUCED BUOYANCY

B.P. HUYNH **AND** **R.I. TANNER**

DIVISION OF ATMOSPHERIC RESEARCH
CLOUD PHYSICS LABORATORY
EPPING N.S.W. 2121 AUSTRALIA

DEPARTMENT OF MECHANICAL ENGINEERING
UNIVERSITY OF SYDNEY
SYDNEY, N.S.W. 2006 AUSTRALIA

SUMMARY A finite element scheme has been developed to investigate problems of fluid flows and heat transfer. The problem of free convection in a square cavity is examined. Here the two vertical walls of the cavity are maintained at fixed but different temperatures, while the top and bottom walls are insulated. The resultant flow configurations and heat transfer rates are obtained when the Rayleigh number is varied between 10^3 and 10^5, while the Prandtl number is held constant at 0.71. The results compare favourably with other investigations. The problem of combined free-forced convection in a vertical, circular pipe is also considered. The pipe wall is subjected to constant heat fluxes and the induced buoyancy is allowed to interfere with the already established forced convection configurations. Here it is seen that the dependence of the fluid physical properties on the temperature is the main cause for any significant variations from the isothermal forced convection situations.

1 INTRODUCTION

Some time ago, a finite element computer program was developed to investigate the problems of extrusion and of jet flows (Tanner et al, 1975; Phuoc and Tanner, 1980). Subsequently, it has been expanded to include other coupled fluid flow and heat transfer problems, including those with thermally-induced buoyancy.

In the first part of this report, the problem of free-convection in a (two-dimensional) square cavity is examined. This problem, sometimes called the "double-glazing" problem, is of considerable interest in many practical applications. Examples are in the construction of insulating double walls or glass windows for dwellings, or the dispersion of heat or pollutants in estuaries due to horizontal gradients of heat or salinitres. Here the two vertical walls of a square cavity are maintained at fixed but different temperatures, while the top and bottom walls are insulated. The resultant flow configurations and heat transfer rates across the cavity are obtained when the Rayleigh number is varied between 10^3 and 10^5, while the Prandtl number is held constant at 0.71, which corresponds to air properties in normal conditions.

In the second part, the problem of combined free-forced convection in a circular, vertical pipe is considered. The working fluid is assumed to be water. The pipe wall is subjected to constant and uniform heat fluxes, and the induced buoyancy is allowed to interfere with the established forced convection configurations. This situation is relevant to various applications, e.g., in solar collectors and tubular heat exchangers.

These problems are solved numerically by using a finite element scheme based on the Galerkin discretisation procedure. This scheme has been fully described elsewhere (Tanner, et al, 1975; Phuoc and Tanner, 1980).

2 FREE-CONVECTION IN A SQUARE CAVITY

2.1 General Remarks

This problem has been extensively investigated by many authors (Batchelor, 1954; Elder, 1965; Grill, 1966; Jones and Thompson, 1981; De Vahl Davis and Jones, 1981; Quon, 1981; Lee and Korpela, 1983; etc.). It has been pointed out that there are three independent non-dimensional parameters which uniquely determine the solution (Batchelor, 1954). This can be seen by a dimensional examination of the governing equations and boundary conditions. These three parameters are: (i) the aspect ratio A = (height/width) of the cavity; (ii) the Prandtl number Pr = (kinematic viscosity/thermal diffusivity) of the fluid; and (iii) the Rayleigh number Ra which describes the relative importance of buoyancy forces and diffusive forces.

Here the cavity is assumed to be square (A = 1) and the Prandtl number is fixed at 0.71 (corresponding to air under normal conditions), while the Rayleigh number is varied between 10^3 and 10^5. This work is, in fact, in response to a call for this problem to be made a comparison problem; subsequently, there have been 36 contributions whereby various numerical methods have been used, including finite element methods (Jones and Thompson, 1981; De Vahl Davis and Jones, 1981).

2.2 Governing Equations and Boundary Conditions

The geometry of the flow field and the non-dimensional boundary conditions are shown in Fig. 1, which also shows the grid pattern used for the cases Ra = 10^4 and 10^5. Neglecting the viscous dissipation and assuming Boussinesq approximation, the non-dimensionaled governing equations are:

$$\text{conservation of mass:} \quad \partial v_j/\partial x_j = 0; \tag{1}$$

$$\text{conservation of momentum:} \quad \partial t_{ij}/\partial x_j - v_j\, \partial v_i/\partial x_j + f_i = 0; \tag{2}$$

$$\text{conservation of energy:} \quad \partial^2 T/\partial x_j\, \partial x_j - v_j\, \partial T/\partial x_j = 0 \tag{3}$$

where v_i is the velocity component in the x_i direction, T temperature and t_{ij} the stress tensor; here the body force vector is given by

$$\begin{Bmatrix} f_i \end{Bmatrix} = \begin{Bmatrix} \text{Ra. Pr.T} \\ 0 \end{Bmatrix}.$$

where the static pressure term due to gravity has also been neglected.

These equations, together with the boundary conditions shown in Fig. 1, are now solved by the finite element method mentioned above.

2.3 Results and Discussion

(a) General results

In general, our results are in good agreement with other works when applicable. See, e.g., De Vahl Davis and Jones (1981), Jones and Thompson (1981). Section (b) below shows the summary of our main results.

Two different grid patterns are used. The grid pattern used for Ra = 10^3 is a simple 6 × 6 regularly-spaced square grid (in terms of elements this would be a 5 × 5 element problem). The grid pattern used for Ra = 10^4 and 10^5 is a 9 × 9 grid shown in Fig. 1. For the latter grid pattern, an attempt is made to take advantage of the previously known results to allocate more, finer elements to regions of larger gradients.

Figs. 2a-c and 3a-c show the computed contours of the stream function, temperature and pressure for the two cases Ra = 10^4 and Ra = 10^5.

The flow configurations show a progressive transition from the conduction regime to the boundary-layer flow regime as Ra increases, and the development of a multi-cellular flow pattern occurring at a value of Ra between 10^4 and 10^5. The temperature field also shows a progressively thinning thermal boundary-layer with increasing Ra.

The contours in Figs. 2c and 3c show the relative values of pressure within the flow field. It has been found that the relative difference Δp between the maximum and minimum pressure values varies linearly (on a log.log scale) with respect to Ra. Thus Δp increases from 524.4 at Ra = 10^3, to 4704.5 at Ra = 10^4, and to 42191.1 at Ra = 10^5. This linear relationship is similar to that between the average Nusselt number Nu and Ra, where

$$\overline{Nu} = \int_0^1 \left| \left(\frac{\partial T}{\partial x} \right)_{x=0} \right| dz$$

is a dimensionless quantity describing the heat transfer across the cavity.

(b) Summary of main results

Table 1 below shows our main results for the cases of Ra = 10^3, 10^4 and Ra^5. Unfortunately, higher values of Ra were not considered due to high costs.

Here u,w are velocity components in the x,z directions respectively, χ is the stream function, and the local Nusselt number Nu is defined to be $Nu = (\partial T/\partial x)_{x=0}$.

Generally, despite the coarse grid patterns used, our results compare favourably with those of other authors who have used much finer grid patterns. More details about the individual numerical methods and mesh sizes, etc. can be seen in the Jones and Thompson's (1981) report or De Vahl Davis and Jones' (1981) summarizing paper.

3 COMBINED FREE-FORCED CONVECTION IN A CIRCULAR VERICAL PIPE

3.1 General Remarks

The problem of combined free-forced convection in a circular pipe has been studied by, e.g., Zeldin and Schmidt (1972), Christionsen and Shinohara (1976), Collins et al (1977, 1980).

Here, using a finite element method, this problem is investigated with the fluid physical properties allowed to be temperature-dependent in some cases (Cases 3 and 3a), so that comparisons can be made with cases (1 and 1a) where the flow is purely forced convection with zero buoyancy, and with cases (2 and 2a) where the temperature change is assumed to affect only the buoyancy force but does not influence other physical properties of the fluid. This type of comparison does not seem to have been considered before.

It is believed that the large discrepancies between theoretical predictions and experimental evidence encountered by workers investigating, for example, the thermosyphon flows in solar collectors (Morrison and Ranatunga, 1980), are due mainly to the misrepresentation of the flow structures and the temperature profiles in the collector pipes, usually due to neglect of the variation of fluid physical properties with temperature. Thus one main purpose of this study is to see to what extent the inclusion of temperature-dependency of the physical properties will affect the flow field.

3.2 Governing Equations and Boundary Conditions

It is assumed that the fluid is Newtonian and the flow has already reached steady state conditions. The governing equations of the flow field are again those of continuity, momentum and energy, applicable to an axisymmetric situation. Here however, unlike the non-dimensionalised equations (1)-(3), the viscous dissipation term is included in the energy equation, and the governing equations are kept in their dimensionalised forms.

We base our basic data on those given in experiment A by Morrison and Ranatunga (1980). Thus the working fluid is water, pipe radius R = 0.55 cm, flow rate Q = 3.68 cm^3/s giving a mean velocity $\bar{w}$ = 3.872 cm/s and a Reynolds number at inlet $Re_o \doteq 479$. However, unlike in their experiment where the pipe length is 110 cm, here for practical computing reasons, we limit the pipe length to a value Z = 11 cm for three cases, and 20.46 cm for three others.

Three sets of cases are considered here:

(i) Cases 1 and 1a: Temperature change has no effect at all on the kinematics.

(ii) Cases 2 and 2a: Boussinesq approximation is applicable so that the density change due to temperature affects the buoyancy force terms only but does not affect the inertia terms. Otherwise, the flow is incompressible and other physical properties of the fluid are kept constant.

(iii) Cases 3 and 3a: Boussinesq approximation is also applicable, but temperature change also affects other fluid physical properties such as viscosity η, thermal conductivity k and the coefficient of thermal expansion β. The variations of η, k and β are as appropriate to water. However, fluid density and thermal capacity are assumed to be always constant.

The boundary conditions are as shown in Fig. 4. In addition, the following conditions are also applied:

(i) For Cases 1, 2 and 3, maximum pipe length is Z = 11 cm; a fully developed parabolic velocity profile is prescribed at inlet, i.e. $w = 2\bar{w}(1-(r/R)^2)$ cm/s; and $\partial T/\partial r = 2.6307 \times 10^6/k$ °C/cm along the pipe wall, corresponding to 100 W of thermal energy applied over the length of 110 cm of pipe.

(ii) For Cases 1a, 2a and 3a, maximum pipe length is Z = 20.46 cm; a uniform velocity profile is now applied at inlet, so that $w = \bar{w}$ = 3.872 cm/s; and $\partial T/\partial r = 2.63.7 \times 10^5/k$ °C/cm along the pipe wall.

3.3 Results and Discussion

(a) Grid patterns

The grid pattern used in Cases 1, 2 and 3 is an 8 × 48 grid (8 grid points in the radial direction, 48 in the axial direction), whereas that used in Cases 1a, 2a and 3a is a 10 × 99 grid. The arrangement is such that as the temperature increases with the axial distance, the finite elements subdividing the flow field are more refined. Also, smaller elements are allocated close to the wall where temperature gradients are largest.

(b) Velocity distribution

(i) Cases 1, 2 and 3. It has been found that the profiles for Cases 1 and 2 are almost identical; at

TABLE I

NATURAL CONVECTION RESULTS

Ra	10^3	10^4	10^5
Nu	1.13	2.22	4.08
Nu_{max} (@ z)	1.50	3.51 (0.15)	7.28 (0.076)
Nu_{min} (@ z)	0.68 (1.0)	0.46 (1.0)	0.47 (1.0)
u_{max} (@ z) on x = 0.5 plane	3.67 (0.80)	16.22 (0.80)	35.46 (0.86)
w_{max} (@ x) on z = 0.5 plane	3.70 (0.20)	19.51 (0.14)	72.18 (0.070)
χ (0.5, 0.5)	1.03	5.17	8.83
χ_{max} (x, z)	1.03 (0.5, 0.5)	5.17 (0.5, 0.5)	9.50 (0.28, 0.56)

outlet (z = 11 cm or 20R) the centre line value of the axial velocity of Case 2 is smaller than that of Case 1 by less than 0.1%. However, at this same location, Case 3 shows a much more substantial difference, as shown in Fig. 5. From this figure, it can also be projected that by the end of the full pipe length used in Morrison and Ranatunga's experiment (z = 110 cm or 200R), the centre line value of the axial velocity would be about 17% less than the parabolic (inlet) value, whereas near the wall (at r = 0.96R) its value would be about 16% higher. It is clear that these deviations are quite substantial.

(ii) Cases 1a, 2a and 3a. Again, like Cases 1 and 2, it has been found that there is practically no difference in the velocity profile between Cases 1a and 2a. Case 3a, however, shows some deviation from the other two cases, although this deviation is also small due to a ten-fold reduction in the heat transfer rate; at outlet (z = 20.46 cm or 37.2R), it is only about 1.5%. The axial velocity profiles of Cases 1a and 2a are shown in Fig. 6.

(c) Pressure distributions

It has been found that, buoyancy alone practically does not effect the pressure distribution along the pipe. However, the allowance for variable physical properties (Cases 3 and 3a) has introduced a large reduction in the pressure head required. For examples, from Case 3, this reduction is up to about 20% of the Poiseuille value over a distance of 20R; whereas the pressure from Case 3a is about 9% below that of Cases 1a and 2a, at pipe outlet (z = 37.2R).

4 CONCLUSION

It has been shown that the finite element scheme developed earlier for quite a completely different class of problems can also be successfully applied to problems involving buoyancy effects.

In the problem of free convection in a square cavity, despite the rather coarse grid patterns used, the results presented here are generally in good agreement with published results by other authors, particularly regarding the more interesting aspects of the solutions such as the flow configurations, temperature distributions and heat transfer rates.

It should also be mentioned that all the solutions show very good centro-symmetry in accordance with the Boussinesq approximation, and with the symmetry of the flow domain and boundary conditions.

On the problem of combined free-forced convection in a circular, vertical pipe, it is interesting, although not surprising, to see that it is the dependence on temperature of the physical properties, coupled with the buoyancy effect, that causes most of the variations from the isothermal configurations in the velocity profiles and the axial pressure distributions.

The buoyance effect alone hardly causes any significant departure from the isothermal case.

5 REFERENCES

BATCHELOR, G.K. (1964) Heat transfer by free convection across a closed cavity between vertical boundaries at different temperatures. Quart. Appl. Math., 12 (3). 209-233.

CHRISTIANSEN, E.B. and SHINOHARA, T (1976) Combined forced and natural convection entrance region heat transfer. Canadian J. of Chem. Engg., 54, 626-630.

COLLINS, M.W. (1980) Finite difference analysis for developing laminar flow in circular tubes applied to forced and combined convection. Int. J. for Num. Meth. in Engg., 15, 381-404.

COLLINS, M.W., ALLEN, P.H.G. and SZPIRO, O. (1977) Computational methods for entry length heat transfer by combined laminar convection in vertical tubes. Proc. Instn Mech. Engrs., 191, 19-29.

DE VAHL DAVIS, G. and JONES, I.P. (1981) Natural convection in a square cavity - a comparison exercise. Proc. 2nd Intern. Conf. Numerical Methods in Thermal Problems, Venice, Italy (in press).

ELDER, J.W. (1965) Laminar free convection in a vertical slot. J. Fluid Mech., 23 (1), 77-98.

GILL, A.E. (1966) The boundary-layer regime for convection in a rectangular cavity. J. Fluid Mech., 26 (3), 515-536.

JONES, I.P. and THOMPSON, C.P., Editors (1981) Numerical solutions for a comparison problem on natural convection in an enclosed cavity. U.K. Atomic Energy Authority, Harwell Report AERE-R 9955, AERE, Harwell, HMSO, U.K.

LEE, Y. and KORPELA, S.A. (1983) Multicellular natural convection in a vertical slot. J. Fluid Mech., 126, 91-121.

MORRISON, G.L. and RANATUNGA, D.B.J. (1980) Thermosyphon circulation in solar collectors, Solar Energy, 24, 191-198.

PHUOC, H.B. and TANNER, R.I. (1980) Thermally-induced extrudate swell. J. Fluid Mech., 98 (2) 253-271.

QUON, C. (1981) Effects of grid distribution on the computation of high Rayleigh number convection in a differentially heated cavity. Paper presented at 2nd National Symp. on Numerical Meth. in Heat Transfer, Sept. 28-30, Univ. of Maryland, U.S.A.

TANNER, R.I., NICKELL, R.E. and BILGER, R.W. (1975) Finite element methods for the solution of some incompressible non-Newtonian fluid mechanics problems with free surfaces. Comp. Meths. in Appl. Mech. & Engg., 6 (2), 155-174.

ZELDIN, B. and SCHMIDT, F.W. (1972) Developing flow with combined forced-free convection in an isothermal vertical tube. J. Heat Transf., Trans. of the ASME, 94, 211-223.

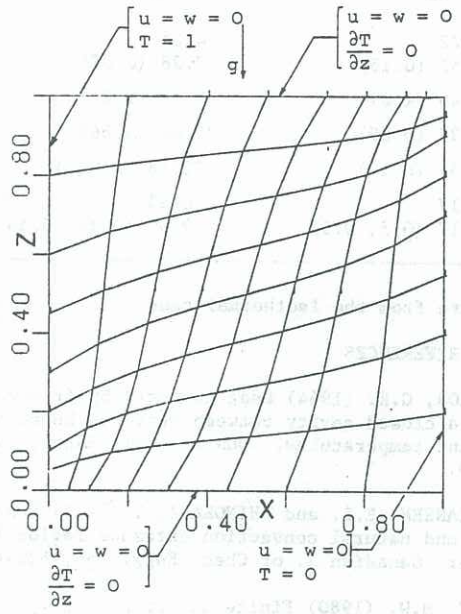

Figure 1 Problem of free convection in a two-dimensional square cavity: Geometry of the flow field, non-dimensional boundary conditions and grid pattern for Cases Ra = 10^4 and 10^5. The grid pattern for Case Ra = 10^3 is a simple 6 × 6 regularly-spaced square grid (or 5 × 5 elements).

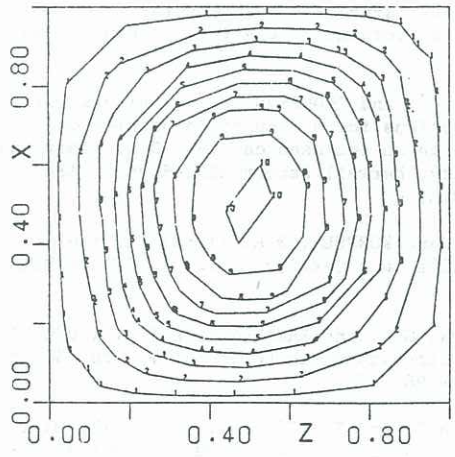

Figure 2a Streamlines for Case Ra = 10^4

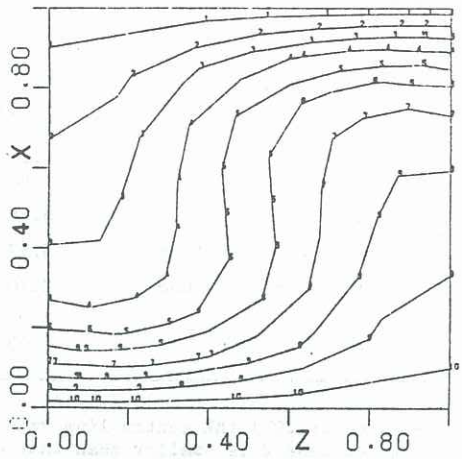

Figure 2b Isotherms for Case Ra = 10^4

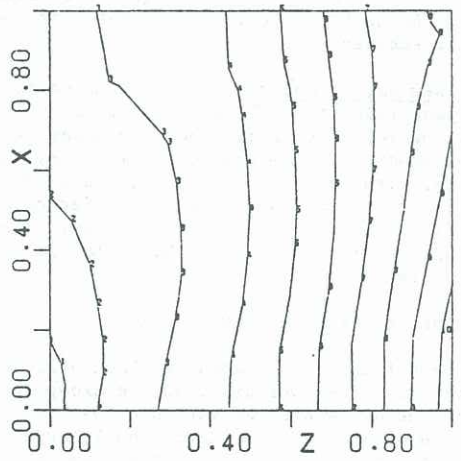

Figure 2c Isobars or contours of pressure for Case Ra = 10^4. Contour interval is 470.5.

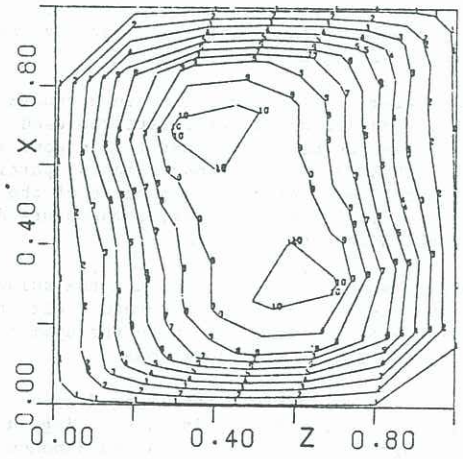

Figure 3a Streamlines for Case Ra = 10^5

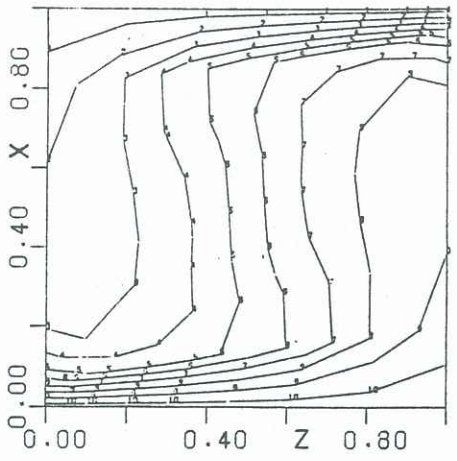

Figure 3b Isotherms for Case Ra = 10^5

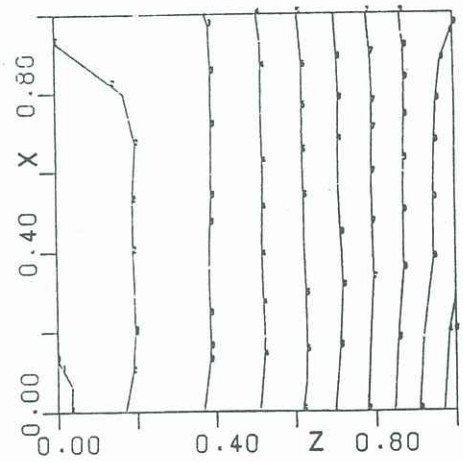

Figure 3c Isobars or contours of pressure for Case Ra = 10^5. Contour interval is 4219.1.

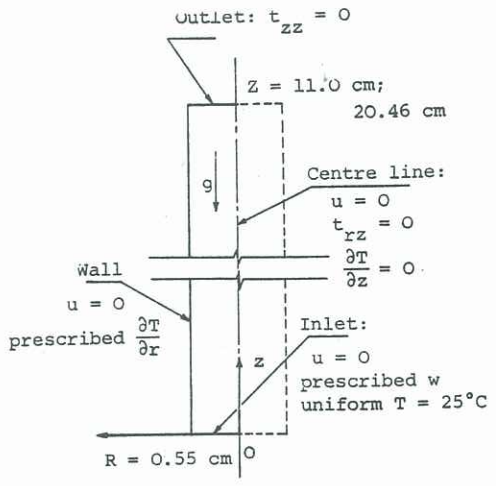

Figure 4 Problem of combined free-forced convection in a circular, vertical pipe: Geometry of the flow field and boundary conditions.

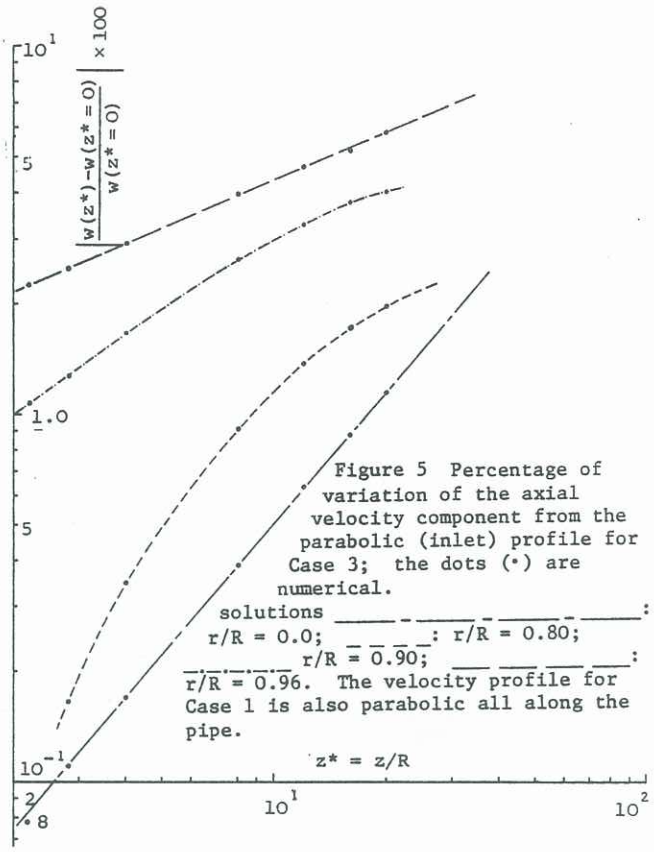

Figure 5 Percentage of variation of the axial velocity component from the parabolic (inlet) profile for Case 3; the dots (•) are numerical. solutions _____ - _____ - _____ - _____: r/R = 0.0; _ _ _ _ _: r/R = 0.80; _._._._._ r/R = 0.90; ___ ___ ___ ___: r/R = 0.96. The velocity profile for Case 1 is also parabolic all along the pipe.

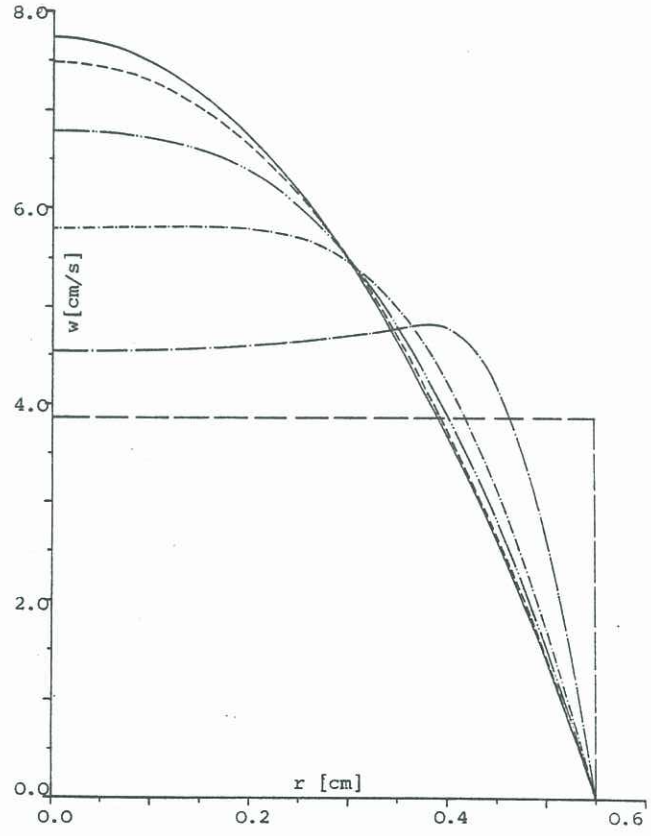

Figure 6 Developing profiles for Case 1a and 2a. _____ _____ _____: z/R = 0 (inlet); _____._____._____: z/R = 1.64; _._._._._._: z/R = 8.0; _____.._____: z/R = 18.0; ____: z/R = 37.20 (outlet). For comparison, the parabolic profile is also shown, as _____ .